Eur. Radiol. 8, 1148–1159 (1998)

Review article

Mediastinal masses: diagnostic approach

F. Laurent, V. Latrabe, R. Lecesne, H. Zennaro, J. Y. Airaud, J. F. Rauturier, J. Drouillard

Service d'Imagerie Médicale, Radiologie Diagnostique et Thérapeutique, Hôpital Haut Lévêque, CHU de Bordeaux, Avenue de Magellan, F-33 604 Pessac, France

Received 20 May 1997; Revision received 15 September 1997; Accepted 24 December 1997

Abstract. In most clinical situations the modern radiological approach to a mediastinal mass consists of performing a CT scan following the chest radiograph. Magnetic resonance imaging is indicated when CT findings are equivocal and as the first-line method in particular situations such as suspected involvement of the posterior mediastinum. In both techniques, tissular components of the mass assessed by density or signal intensity analysis, together with the precise location, are the leading edge of the radiological diagnosis. This review deals mainly with the differential diagnosis of primary neoplasms according to CT and MRI findings.

Key words: Mediastinum – CT – MRI

Introduction

Radiological evaluation of a mediastinal mass is an important challenge in chest radiology. Whereas plain film gives limited results, cross-sectional techniques, especially CT and MR, play a powerful role in evaluating the mediastinum. Presently, a specific diagnosis is often possible; if not, at least a limited differential diagnosis can be made.

General considerations

According to two large series, the most frequent lesions encountered in the mediastinum are thymoma, neurogenic tumors, and benign cysts, altogether representing 60 % of patients with mediastinal masses [1, 2]. However, significant differences exist between adults and children. Neurogenic tumors, germ cell neoplasms and foregut cysts represent 80 % of childhood lesions, whereas primary thymic neoplasms, thyroid masses and lymphomas are the most frequent in adults [1–3].

Most patients with mediastinal lesions are usually chronically asymptomatic. Eighty-three percent of incidentally discovered masses are benign and 57 % of those seen in symptomatic patients are malignant [1]. Symptoms can include dyspnea, dysphagia, cough from airway compression, superior vena cava syndrome, hoarseness from laryngeal nerve involvement, or symptoms resulting from spinal cord compression. Myasthenia gravis or, less frequently, Cushing's syndrome can also reveal mediastinal masses. Approximately one third of mediastinal masses are malignant and invasion or obstruction of nearby structures on imaging studies is suggestive of malignancy [4–6].

Imaging modalities

Chest radiographs

Posteroanterior and lateral chest radiographs are the first imaging modalities used when a mediastinal mass is suspected. Deformation of mediastinal contours and lines and/or displacement of normal structures must be present to identify a mass. Tissular characterization is limited. Typical location and findings can help in identification in lymph nodes and vascular masses, and may suggest a limited differential diagnosis on the basis of age, gender, and clinical findings [7, 8].

Computed tomography

Computed tomography is the most important tool in the evaluation of a mediastinal mass. It is the next step following chest radiography and is often sufficient in the management of the patient. Characterization on CT is based on specific attenuation of air, fat, water, and calcium. Vascular abnormalities and the degree of vascularization of soft tissue masses are demonstrated by dy-

Correspondence to: F. Laurent

namic incremental CT or spiral CT more recently [9, 10]. Precontrast slices are performed first. Contrast-enhanced slices of adapted thickness to the size of the lesion are then obtained. Reconstruction interval near the half of the slice thickness is suitable for 3D or multiplanar reconstructions. Multiplanar reformations are a valuable adjunct and more useful in clinical practice than 3D reconstructions.

Magnetic resonance imaging

Magnetic resonance imaging has many advantages in imaging the mediastinum, e. g., excellent soft tissue contrast with spontaneous tissue–vessel contrast and direct multiplanar capabilities. The MRI technique includes currently ECG-gated spin-echo and T2-weighted and gadolinium-enhanced T1-weighted scans in the appropriate axial, sagittal, coronal, or oblique plane. Gradient-echo techniques are useful in the exploration of vascular patency. In clinical practice MRI is used when iodine contrast cannot be used, or after CT if questions remain unanswered. Identification of some cystic lesions as well as assessment of preoperative relationships with the pericardium, heart cavities, spinal cord, and canal are common indications and in some situations vascular involvement [11–13].

Ultrasound and other imaging techniques

Transthoracic US is not currently used in mediastinal mass evaluation, although it does have a potential role in certain situations. The major limitation is an inadequate window, but useful information can be obtained especially in children in masses abutting the chest wall and in vascular abnormalities [14]. Endesophageal ultrasonography may have some interest in assessing masses of the posterior mediastinum, particularly to evaluate their relationships with esophagus or left atrium. Esophagogram and endoesophageal US are useful when questions are raised about the esophageal origin of the mass. Both spiral CT and MRI have led to a more reduced utility of vascular opacification techniques that are employed presently.

Transthoracic needle biopsies

Invasive diagnostic procedures often play a valuable part in staging and providing tissue for pathological study in order to plan treatment. Mediastinoscopy and parasternal mediastinotomy have traditionally filled this role. Percutaneous fine-needle aspiration and, more recently, core biopsies with large bore needles guided by CT scanning or US have also been advocated for the diagnostic examination of mediastinal lesions [15, 16]. A preoperative histological diagnosis is unnecessary if the mass seems reasonably resectable. Conversely, if the mass is clearly invasive and looks unresectable, then a biopsy, either guided by imaging or surgical, is indicated. Despite the excellent safety and low complication rate with guided biopsies, some authors believe that the nature of the common tumors found especially in the anterosuperior compartment tends to limit the accuracy of guided biopsies, especially when classification is needed like in non-Hodgkin's lymphoma, thymomas, or Hodgkin's disease. In such indications the role of CT-guided biopsies depends on the importance placed on them by radiologists, pathologists, and surgeons.

Diagnostic approach of mediastinal masses

Differential diagnosis of mediastinal masses

When a central mass is discovered on a chest radiograph, the first step is to be sure that this mass arises within the mediastinum, rather than from contiguous lung, pleura, or chest wall. Masses that lie deep to mediastinal vessels are clearly mediastinal in origin, and those from the sternum or spine are easily identified on CT. With a few exceptions, a mass with a spiculated, nodular, or irregular edge arises in the lung, and a mass with a broad base on the mediastinum and a smooth edge arises in the mediastinum or mediastinal pleura. A normal remaining pleura is strongly in favor of a mediastinal origin. Using these criteria, 99% of masses may be correctly localized to the lung, pleura, or mediastinum [17].

The second step is to recognize abnormal radiographic findings related to anatomical variants such as aortic-arch abnormalities, masses arising from the digestive tract (hiatal herniae, esophageal masses). In clinical practice CT can only be avoided in cases of typical hiatal herniae. Esophageal masses and abnormalities are not usually discussed with mediastinal masses despite the fact that they belong to the mediastinum.

In this review we focus on primary mediastinal tumors. Vascular anomalies and mediastinal lymph nodes are briefly mentioned in the following:

1. Vascular anomalies represent approximately 10% of mediastinal masses. They must be correctly recognized since failure to identify an aneurysm can lead to a dramatic event during an invasive diagnostic procedure.
2. Mediastinal lymph nodes certainly represent the most common cause of mediastinal masses. They are often easily recognized on chest film, and if not, they are recognized on CT, and are uncommonly confused with primary tumors. Discussion of their most common etiologies, e. g., metastasis of solid tumors and lymphomas, is beyond the scope of this article.

Classification of mediastinal masses

The radiological compartmentalization of the mediastinum in anterior, middle, and posterior compartements introduced by Felson helps in focusing the differential diagnosis of masses on the basis of their site. However,

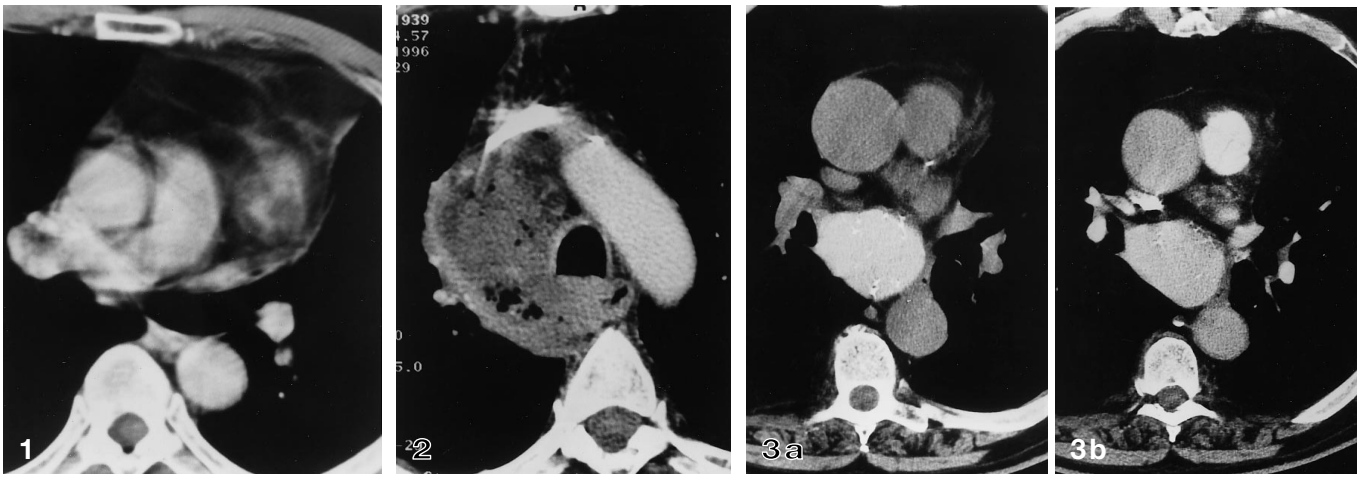

Fig. 1. Liposarcoma. Large mass of the retrosternal prevascular space mainly composed of fatty tissue with septations and a central nodule

Fig. 2. Mediastinal abscess after laryngeal perforation. Laterotracheal fluid collection with gas bubbles

Fig. 3 a, b. Bronchogenic cyst. **a** Non-enhanced CT: subcarinal high-attenuation mass (89 HU). Small calcifications within the mass. **b** No enhancement after IV contrast injection

many tumor types can be found in any of the three compartments [7, 8].

Attenuation values at CT and signal intensity at MRI give much more detailed information than chest film concerning the tissular composition of the mass. Chest radiography is only able to identify calcifications, although in some cases a fatty component can be suspected as a zone of relative radiolucency. The diagnosis can be at least partly suggested based on the major component of a mass: fatty, cystic, or solid tissue. In most cases calcifications and their patterns are not as useful in the differential diagnosis. Additional information can also be obtained from the degree and type of vascularity of the lesion due to contrast enhancement on CT or MRI [9, 10].

Presently, tissue components, as shown by CT or MR scans, together with size, shape, and precise location according to the compartments described by Heitzman [8], are the leading edge of the diagnosis of a mediastinal mass. In the following, we successively consider mediastinal masses of predominant fatty, cystic, and solid tissular components. Among the latter, those with an atypical attenuation are considered separately.

Fatty masses

Fat is specifically recognized by its low CT numbers, which vary from –70 to –130 HU for pure fat. Fat is normally present in the mediastinum and increases with age. Normal fat is unencapsulated and does not affect the normal contours of the mediastinum. On MR well-differentiated fat has a high signal intensity on both T1- and T2-weighted sequences, identical to subcutaneous fat. In the majority of cases, discovery of the fatty nature of a mass indicates benignancy. True lipomatous tumors are much less common than herniation of abdominal fat or diffuse lipomatosis.

Mediastinal diffuse lipomatosis is an overabundant amount of histologically normal fat resulting in smooth mediastinal widening on chest radiographs. Its roentgenographic density is often less than that of other masses. Locations of this overaccumulation of fat are the upper mediastinum, the cardiophrenic angles, and less frequently, the paraspinal areas which can widen the spinal line. Homogeneity and absence of compression of surrounding structures differentiate this benign condition from multiple lipomas. This condition may be part of a generalized obesity but not exclusively, or is seen in patients suffering from Cushing's disease or those treated with steroid therapy [18].

Omental fat can herniate through the foramen of Morgagni or Larrey and create the appearance of a cardiophrenic angle mass. Esophageal hiatus herniations of perigastric fat extend along the aorta or may appear as a retrocardiac mass. Connections with abdominal fat may be easily demonstrated by multiplanar reconstruction with CT. Magnetic resonance imaging, although not indicated, is able to demonstrate abdominal fat on sagittal and coronal acquisitions.

Mediastinal lipomas and liposarcomas represent only 1 % of all primary mediastinal tumors. They do not produce compressive symptoms unless they are large enough. The modling to the mediastinal contour can be so marked that a large lipoma may mimick a cardiomegaly. In contrast, liposarcomas show unhomogeneity of the fat and contain large areas of soft tissue density (Fig. 1). They are often locally invasive at the time of the diagnosis. Sometimes, fat is no longer detectable within the tumor and is only visible on histological samples [19].

Tumors other than lipomas may contain some fat. Among tumors predominantly composed of fat, thymolipomas are the most common. Usually of large volume, these tumors develop in the thymic space. Especially when they are large, they may extend downwards on the diaphragm, leaving the superior mediastinum relatively clear, as the result of their soft and pliable consis-

tency. They are composed of a mixture of fatty and tissular components [20].

Most teratomas are cystic; however, some may contain a small amount of fatty tissue which clearly indicates their origin [9, 10]. Other uncommon lesions that may contain some fat include hemangiomas, angiolipomas [21], lipoblastomas in infants [22], and extramedullary hematopoiesis [23]. Fatty tissue component may be part of a complex mesenchymal sarcoma with various tissues of mesenchymal origin, i.e., fibrous, osseous, or vascular components [24].

Cystic masses

Primary cysts represent 15–20% of all primary mediastinal masses. Most of them do not produce symptoms and become large before they are discovered, usually as an incidental chest radiographic finding. Because of their tendency to enlarge or become infected, surgical excision is usually recommended.

True cystic lesions should be differentiated from the cystic degenerative changes observed in many solid tissular tumors, nodes, and from abscesses and hematomas. Areas of low attenuation may be present secondary to necrosis, old hemorrhage, or the intrinsic properties of the neoplasm. On CT identification of these degenerative cystic changes is based on the visualization of an unhomogeneous low-density mass with thick wall, sometimes in conjunction with other CT findings, such lymphadenopathy, pulmonary, or pleural abnormalities. Goiters, thymomas, cystic teratomas, nerve root tumors, seminomas, and enlarged nodes from any origin may show such a finding [25]. Hodgkin's disease and other lymphomas can also be associated with cystic changes before or after treatment [9, 10]. Mediastinal abscess shows a low-attenuation mass surrounded by an enhancing rim and sometimes are filled in with gas or air–fluid level and therefore are not confused with a true cystic mass. Clinical features and associated CT findings, such as gas bubbles, or communication with an empyema, usually permit differentiation from true cysts (Fig. 2). Subacute or chronic hematomas may appear as low-attenuation masses, occasionally with a fluid–fluid level. Pseudomasses with water densities include fluid-dilated esophagus or pericardial recesses easily identified at CT.

Typical cysts appear on chest radiograph as smooth, sharply marginated mediastinal lesions. On CT they have a similar attenuation to that of water and do not enhance. Their margins are well defined and their wall is barely perceptible. Any cyst may have a higher attenuation than that of water due to its calcic, proteinaceous, mucus, or hemorrhagic content. Such lesions may be undistinguishable from solid soft tissue neoplasms, although the complete absence of enhancement after administration of IV contast material may be a clue to their recognition [9, 10, 26]. However, lack of enhancement is sometimes difficult to ascertain near the heart for example. On MRI typical cysts have a high signal intensity on T2-weighted images, but show a variable T1-weighted appearance. Those filled in with serous fluid have a low signal intensity and those with a viscous proteinaceous or bloody content have a signal which varies from intermediate to very high intensity. No enhancement after gadolinium chelate injection is a useful additional feature to assess the cystic composition [27].

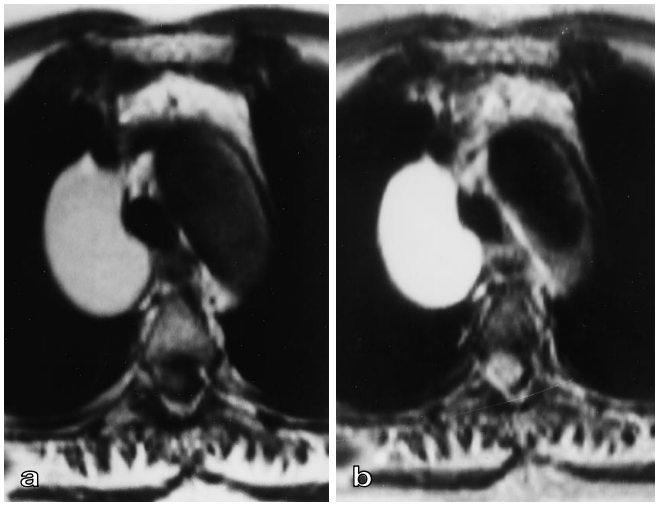

Fig. 4a, b. Bronchogenic cyst MRI laterotracheal mass without perceptible wall. High signal intensity on both **a** T1-weighted and **b** T2-weighted images

Most mediastinal cysts are developmental in origin and, according to the type of epithelium of their wall, include bronchogenic, esophageal duplication, neuroenteric cysts, grouped together under the generic term of foregut cyts, and pericardial cysts; however, this distinction is not always clear. Thymic cysts may be congenital but their pathophysiology may be more complex including acquired cysts.

Bronchogenic cysts have a fibrous capsule, often contain cartilage, are lined by respiratory epithelium, and contain mucoid material that is remarkably viscid. The clinical features are variable from respiratory distress in infants to asymptomatic status in older children and adults. They are stable in size except when complicated by infection or hemorrhage [28, 29]. They do not usually communicate with the bronchial tree, unlike intraparenchymal cysts. Most of them are located adjacent to the major airways along the paratracheal wall, near the carina, or in the posterior mediastinum. Half of them are of water density and the others have a CT density which varies depending on the cyst content. On rare occasions bronchogenic cysts show an extremely high density related to a milk of calcium content (Fig. 3). Curvilinear calcification of the wall is possible. At MRI bronchogenic cysts frequently show a signal intensity higher than that of muscle on T1-weighted images (Fig. 4a) due to their high proteinaceous content [30–32]. In rare situations a fluid–fluid level has been demonstrated [33, 34]. The signal intensity on T2-weighted images is very high, suggesting a cystic lesion (Fig. 4b). Because this finding may be seen in some solid tumors, gadolinium injection is recommended. Duplication cysts are indistinguishable from bronchogenic cysts, except for their location usually close to the esophagus, sometimes

Fig. 5. Pericardial cyst. Unenhanced CT. Mass of the right anterior cardiophrenic recess of water attenuation

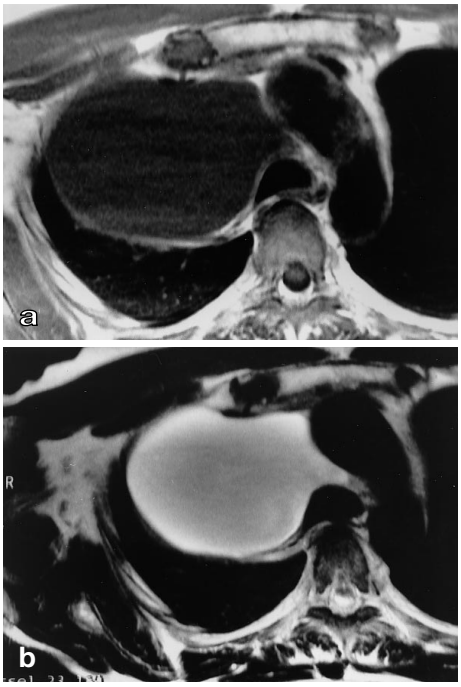

Fig. 6 a, b. Cystic lymphangioma. MRI: large homogeneous laterotracheal mass, extending within the precarinal space, of low signal intensity on **a** T1-weighted and of high signal intensity on **b** T2-weighted images

within its wall. Neuroenteric cysts are rare lesions which may be connected to the meninges through a midline defect in one or more vertebral bodies. The vertebral anomaly (hemivertebrae, butterfly vertebra, or spina bifida) may be located above the level of the cyst. Their communication with the subarachnoid spaces may be demonstrated by MRI which presently replaces CT myelography.

Pericardial cysts are the result of anomalous outpouchings of the parietal pericardium in contrast with pericardial diverticula that communicate with the pericardial sac. Most pericardial cysts are unilocular. They are commonly located in the right cardiophrenic angle (Fig. 5), although they may occur anywhere in relation to the pericardium: posterior cardiophrenic angle, superior retro-aortic pericardial recess. On imaging studies they are seen as smooth, well-defined, oval or round masses in contact with the heart, without a perceptible wall. In some cases an oval shape with a pointed border may be seen [9, 10, 35]. Such cysts may be large. Rapid change in size related to the position suggests a diverticulum rather than a cyst.

Two pathogenetically distinct forms of thymic cysts are described. A congenital one, which tends to be unilocular, derives from remnants of the thymopharyngeal duct. It occurs anywhere along the course of the embryonic thymus gland from the angle of the mandible to the manubrium. Apart from their characteristic water density, calcification has been reported.

Thymic cysts can also be acquired lesions which tend to be multilocular following thymic inflammation. They are known to occur occasionally in patients with mediastinal Hodgkin's disease. Their histogenesis is controversial. They can encountered tissues either on presentation or at recurrence. They may be treatment related or due to thymic infiltration by lymphomatous tissues. The natural history of these thymic cysts is not known. Careful observation with regular follow-up CT scans without additional treatment seems to be the management of choice for residual thymic cysts of mediastinal Hodgkin's disease [9, 10].

Lymphangiomas (cystic hygromas) are tumor-like congenital malformation of the lymphatic system, consisting of lymph channel or cystic lymph spaces lined by endothelium. Their walls are formed by fibrous tissue and smooth muscle. They vary in size and histology, some showing a capillary or cavernous structure, others taking the form of unilocular or multilocular cysts. They may be difficult to resect and may recur due to their invasive nature. Lymphangiomas are typical when connected with a cervical mass, but they may be isolated in the mediastinum. When confined to the mediastinum, they are usually asymptomatic and may be discovered in children or adults. Fewer than 10 % occur in the posterior mediastinum. In typical cases CTor MRI show a cystic mass sometimes multilocular or septated, which molds or envelops adjacent mediastinal vessels [36, 40]. Unilateral or bilateral effusion may occur and in invasive forms chylothorax is a feature.

Cysts of the thoracic duct and intrathoracic meningoceles are rare cystic lesions of the posterior mediastinum [41]. Lateral intrathoracic meningoceles are a protrusion of the spinal meninges through the intervertebra foramina, and are mostly asymptomatic. They may be seen in association with neurofibromatosis and are sometimes multiple and bilateral. Magnetic resonance imaging is the technique of choice in distinguishing meningoceles from neurogenic tumor (see Figs. 7, 13). It is also the technique of choice in differentiating the connection of the lesion with the subarachnoidal spaces.

Solid tissular masses

Most mediastinal masses in an adult population are solid. Clinical and CT findings including precise location are essential for planning treatment. Invasive proce-

dures, such as percutaneous biopsies, mediastinoscopy, or anterior mediastinotomy are often necessary to obtain a definite diagnosis. The CT technique is often sufficient in distinguishing invasive unresectable tumors from well-defined resectable lesions. In some situations, where resectability remains uncertain, additional information may be brought by MRI or endoscopic US. Among tissular masses, two types of CT attenuation may restrict the differential diagnosis to a limited number of possibilities: the spontaneously hyperattenuated mass and masses with a strong enhancement on enhanced CT.

Fig. 7. Magnetic resonance imaging of meningocele. Large high signal intensity mass communicating with the arachnoidal space

Masses with high attenuation on unenhanced CT

Spontaneous hyperattenuation is an uncommon finding which can be simply defined by a mass which has a higher attenuation than muscles on unenhanced CT [26]. Apart from calcified nodes, or tumor calcifications, and some cysts that have been previously mentioned, this feature is frequently seen in thyroid goiters and recent hematomas.

Mediastinal thyroid goiters usually have a spontaneous attenuation smaller than that of the cervical gland but greater than that of muscle (Fig. 8 a). This finding, however, is highly variable and relates to the iodine content of the goiter [9, 10, 26].

Ninety percent of hematomas have areas of high attenuation during the first 72 h, reflecting the high hemoglobin concentration of clotted blood. At this stage the MR signal intensity is low on T1 and T2. When the hematoma ages, its attenuation decreases at CT in a centripetal fashion creating a low-attenuation peripheral halo that increases over time. At MRI the signal intensity on T1-weighted images increases and gives a more typical appearance of the hemorrhagic content.

Other spontaneously hyperattenuated masses include foreign bodies, fresh clots in aneurysms, residual lymphangiographic contrast material, retained surgical sponges, and orally opacified esophageal diverticula [26].

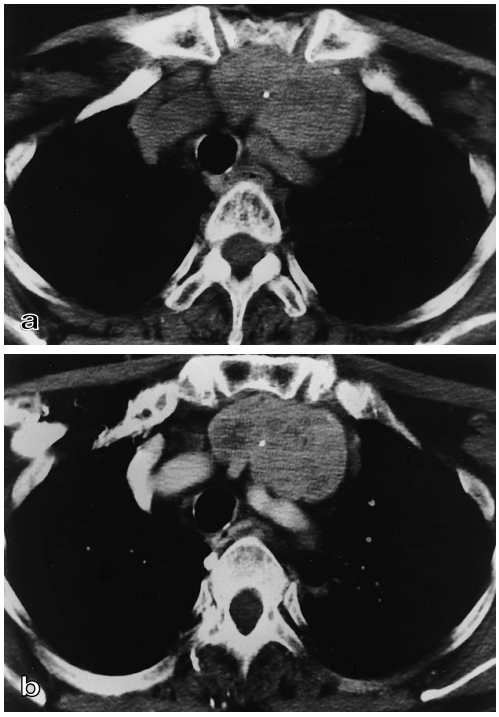

Fig. 8 a, b. Goiter. **a** Plain CT and **b** enhanced CT. Mass of the upper anterior mediastinum spontaneously hyperattenuated compared with muscles

Masses that may highly enhance on CT

Masses that are known to possibly strongly enhance at CT are: goiters, vascular tumors (hemangiomas), parathyroid masses, Castelman disease, medullary cancer of the thyroid, thymic carcinoid, and metastasis of sarcomas and melanomas.

Mediastinal goiters constitute 5–10 % of all resected mediastinal masses. An intrathoracic thyroid mass is usually a benign multinodular colloid goiter or an adenoma and seldomly a carcinoma. Malignant thoracic goiters are not more frequent than their neck counterpart. Small foci of degenerescence are frequent when masive degenerescence remains very seldom. Most patients with thyroid mass are asymptomatic and the abnormality is detected on a routine chest radiograph. Occasionally, symptoms of airway or esophageal compression are present. In most cases thyroid masses represent direct contiguous growth of a goiter into the mediastinum. An intrathoracic thyroid mass developing from heterotopic thyroid tissue without any connection to the thyroid in the neck is extremely rare. Occasionally, the only connection is a narrow fibrous or vascular pedicle not visible at CT. In 80 % of cases, the thyroid extends into the prevascular spaces, but posterior extension behind the brachiocephalic vessels along the trachea represents 20 % of cases. The role of imaging is important in the preoperative assessment of substernal goiters because their surgical approach depends on their precise anatomical location [9, 10]. On plain films they have a well-defined spherical or lobular outline and many displace and narrow the trachea. Tracheal displacement is usually posterior or lateral but may be an-

terior in thyroid masses separating the trachea and esophagus. The combination of findings on CT is characteristic in most instances. Identification of a substernal thyroid tissue is made on the following findings: communication between the cervical thyroid gland and the mass by contiguous slices, mass of unhomogeneous density with cystic and high-density areas, calcifications of various shape, and marked and prolonged contrast enhancement (Fig. 8b) [9, 10]. Occasionally, goiters may compress the brachiocephalic veins or the superior vena cava. Calcifications are more frequently seen the longer the goiter is present. They may be seen in malignant (papillary, follicular carcinomas and medullary carcinomas) as well as benign disease. Limitations in histological specificity similar to sonography for the neck part have been noted with CT and MRI. Distinguishing between benign and malignant goiters at CT is not possible unless the tumor clearly invades beyond the thyroid gland. On MR multinodular goiters have been shown to be relatively hypointense as compared with normal tissue on T1-weighted images, except foci of hemorrhage and cysts that may be hyperintense. T2-weighted images show a typically heterogeneous appearance with high signal intensity throughout most of the gland. Displacement of mediastinal vessels, trachea, esophagus, and relationships between the cervical and thoracic components of the goiter are exquisitely demonstrated by multiplanar imaging whatever the technique, spiral CT or MRI. Radionucleid imaging of the thyroid shows some functioning thyroid tissue in almost all intrathoracic goiters.

Most parathyroid masses are adenomas or hyperplastic glands. They enhance brightly in many cases. Hyperparathyroidism may be caused by parathyroid adenomas that arise in ectopic parathyroid glands in the mediastinum [42, 46]. They may occur in or near the thymus, but an aortopulmonary window location is possible [47]. They are often less than 2 cm in diameter and their detection at CT drops considerably below this size. Technetium-99 Sestamibi SPECT scans have been shown to be more effective in their detection than MRI and CT [48].

Castelman disease (giant lymph node hyperplasia, angiofollicular lymph node hyperplasia) is a variety of lymph node hyperplasia. The hyaline vascular type is seen most frequently as an asymptomatic mass. The plasma cell variety is usually associated with symptoms such as fever, fatigue, anemia and gammaglobulin anomalies. It occurs at any age but frequently in young adults. AIDS and Kaposi sarcomas can be associated and patients may develop a lymphoma. The disease may be confused histologically with lymphoma or thymoma. Vascular neoplasms have been reported to arise in nodes affected by the disease [10]. Well-defined large masses sometimes calcified in the mediastinum or proximal hilum are the radiological features. Multicentric forms have a poorer prognosis and present as multiple enlarged lymph nodes. Striking uniform contrast enhancement is seen on CT or MRI and suggests the diagnosis [49, 51].

Paragangliomas are tumors of the paraganglionic cells and in the chest are chemodectomas or functioning paragangliomas. Chemodectomas are aortic body tumors and are seen as masses of the aortopulmonary window. Functioning paragangliomas occur rarely in the chest and mostly in the posterior mediastinum. These masses are usually extremely vascular and enhance brightly at enhanced CT. At MRI they may show high signal intensity on T2-weighted images. Radio-iodine metaiodobenzylguanidine can show increased activity into the mass and is a good method of identifying any apudoma. If vascular opacification were performed, it would show enlarged feeding vessels [52, 53].

Blood vessel tumors in the mediastinum are rare. Benign lesions are capillary or cavernous hemangiomas according to the size of their vascular spaces. They tend to be well-circumscribed lesions without a true capsule. They typically occur in young patients and may be associated with Rendu-Osler syndrome. Phleboliths, which are potential diagnostic findings, are seen rarely and punctate calcifications may be seen. On enhanced CT they are heterogeneous masses of four distinct patterns of enhancement, in decreasing order of frequency: central, mixed central and peripheral, or peripheral [54]. Mixed lymphatic and blood vessel lesions, such as lymphangiohemangiomas, hemangioendotheliomas, and hemangiosarcomas, are occasionally encountered [24]. Hemangiopericytomas may seldom develop in the chest sometimes arising from the chest wall. They are infiltrative and have a non-specific appearance on CT.

Other solid tissular masses

The most frequent solid masses which arise in the mediastinum enhance less strongly than the vascular structures. Apart from clinical findings, the location of the mass within a mediastinal compartment is the leading thread of the diagnosis. Most commonly, thymic lesions and germ cell tumors occur in the anterior compartments, whereas neurogenic tumors arise in the paravertebral gutter.

Thymic masses

The size of a normal thymus varies strongly with age. Differentiating between a large normal thymus and a small thymic mass can therefore be difficult in children and some young adults. A normal thymus, in contradiction to a thymic mass, conforms to the shape of the adjacent great vessels on CT and MRI. The analysis of the signal intensity at MRI can be useful because normal thymic tissue shows an homogeneous signal, whereas thymic masses often show unhomogeneous signal intensity. Ultrasound can also be used to establish the normality of a prominent thymus in infants, showing an homogeneous low-echo pattern similar to the spleen [9].

Apart from the uncommon cysts, enlargement of the thymus is usually caused by thymomas. Other tumors include malignant lymphoma, thymic carcinoid, and thymic carcinomas.

Thymomas are tumors composed of an admixture of thymic epithelial cells and reactive lymphocytes with a proportion appearing to comprise a continuous spectrum. The predominantly epithelial variety carries the poorer prognosis. On pathologic studies cystic changes are common, in some cases the tumor being almost totally cystic. Calcifications at the periphery of the lesion or throughout its substance, hemorrhage, or necrosis can also be seen. Thymomas vary in size from large masses to small lesions of less than 1 cm in size only detectable on CT. The presence or absence of spread beyond the capsule, rather than the histological appearance within the thymus, determines whether a tumor is labeled benign or malignant by the pathologist: 15–40 % of thymomas turn out to be invasive. Several staging systems are currently used for invasive thymomas with radiation therapy and chemotherapy given in addition to surgical treatment.

Thymomas are seen with equal frequency in men and women at a mean age of 50 years and are extremely uncommon below the age of 20 years. Most patients have no symptoms related to the mass, but thymomas are associated with a large variety of autoimmune diseases notably myasthenia gravis. In patients with myasthenia gravis, a thymoma or a thymic hyperplasia is present in 10–20 % of cases.

Thymic hyperplasia is a term used by pathologists to describe numerous active lymphoid germinal centers in the medulla. The role of CT and MR is limited in detecting this abnormality because 50 % of thymic hyperplasias appear entirely normal on CT, whereas other glands with hyperplasia typically are diffusely enlarged [9, 10, 55–57].

The spectrum of CT findings in patients with thymoma has been extensively described. Non-invasive thymomas appear as round or oval well-circumscribed masses growing asymmetrically to one side of the anterior mediastinum. The CT density is similar to that of a normal young thymus and slightly increases with administration of contrast material. Intratumoral calcifications are seen in one third of cases and areas of cystic degeneration are common. The tumor can occur in the prevascular space of the mediastinum but also around the base of the heart and anywhere between the lower pole of the thyroid gland and the anterior surface of the pericardium [58, 59].

Invasive thymoma appears on CT as an irregular ill-defined mass. They grow along pleural surfaces and can reach the posterior mediastinum and extend downwards along the aorta to involve the crus of the diaphragm and the retroperitoneum. A full CT examination in these patients should extend to the upper abdomen. Pleural extension as droplet spread without continuity with the primary tumor is seen in 15 % of cases. Invasion of the thoracic wall, mediastinal vessels, trachea, pericardium, and lung parenchyma is frequent. Computed tomography is the most precise method for detecting local and regional spread. However, caution should be used to avoid overdiagnosing invasion. Direct contact and absence of cleavage planes are not strictly reliable criteria to predict invasion. On the other hand, clear delineation of fat planes surrounding a tumor should be interpreted as indicating an absence of extensive local invasion [9, 10].

Magnetic resonance imaging has a limited role in the evaluation of thymomas. The MRI signal is only in a few cases helpful for the diagnosis of myasthenia gravis, thymic hyperplasia, and thymic mass. However, vascular and cardiac extension of invasive thymoma is well identified by MRI [60, 61].

Thymic carcinomas are sometimes classified as a subgroup of thymomas. This entity behaves more aggressively and CT features cannot help to distinguish them from invasive thymomas. A local invasion along the pleura or mediastinum, as well as necrosis and calcifications, are frequent [62, 65].

Thymic carcinoid may secrete adrenocorticotropic hormone (ACTH) and present with an ectopic ACTH Cushing's syndrome. The CT features are indistinguishable from thymomas [66].

The thymus in commonly involved in Hodgkin's and non-Hodgkin's lymphomas. Isolated thymic involvement in Hodgkin's disease is much rarer than combined thymic and mediastinal node disease. The major imaging finding is thymic enlargement, being a major differential diagnosis between a large normal thymus and a lymphomatous involvement in young patients [9, 10].

Rebound thymic hyperplasia is a phenomenon in which the thymic gland grows back to a larger-than-normal size after rapid atrophy in response to stress or therapy with antineoplasic or steroids. It has been reported after treatment of lymphomas, Cushing's syndrome, and recovery after a wide variety of other stresses. On CT the appearance is a normally shaped enlarged gland which conforms to the shape of adjacent structures with a similar density to that of the normal gland. The signal at MRI is also similar to normal thymic tissue. Distinguishing between rebound hyperplasia from lymphoma in children and young adults may be very difficult [67–69].

Germ cell tumors

Germ cell tumors arise from tumoral transformation of germinal elements. Sixty percent are benign teratomas that occur with equal frequency in men and women. Malignant varieties have a strong male predominance and include teratocarcinomas, embryonic carcinomas, seminomas, endodermal sinus tumor, choriocarcinomas, and mixtures of these cell types [70, 71].

Benign teratomas usually consist of ectodermal elements such as skin, sebaceous material, hair, and calcification; hence, the expression of dermoid cyst along with smooth muscle and respiratory epithelium. Half the cases are asymptomatic. Others have symptoms caused by local compression, rupture, or infection. Most occur in the anterior mediastinum, but a few are found in the posterior mediastinum. They grow slowly and rapid increase in size may occur because of hemorrhage. Tumors may be uni- or multiloculated. Benign teratomas typically contain a mixture of CT fatty, tissular, and wa-

ter densities (Fig. 9). Fatty and cystic components are present in half the cases, and sometimes a fat–fluid level strongly suggests the diagnosis [72–74]. None of these features are specific for benignity. In cases of rupture within the pleura, a fat–fluid level may also be visible in the pleural space. Calcification in the wall or small spherical or irregular calcifications within the mass, sometimes suggesting dental material, may be seen. Similar information can be obtained with MRI.

The malignant germ cell tumors grow rapidly and metastases may be seen in the lung, pleura, or bone. They secrete beta human chorionic gonadotropin, alpha-fetoprotein, and lacticodehydrogenase which are used to diagnose and monitor the progress of the disease. Malignant germ cell tumors have CT and MR features similar to other primary malignant tumors arising within the anterior mediastinum (Fig. 10). Invasion of mediastinal structures is difficult to assess. Obliteration of fat planes and replacement of mediastinal fat by tumoral tissue is not a formal sign of tumoral involvement since a tumor can only adhere to adjacent structures without invading them. Confirmation of the primary nature of these tumors requires that there is no evidence of testicular or retroperitoneal tumor. The role of imaging modalities is to define disease extent and to monitor response to therapy [71, 75–77]. A residual mass may be seen after successful treatment. This mass may be cystic, representing mature teratoma, and may grow despite being benign [78]. The benign or malignant nature of the mass cannot be stated with certainty on CT criteria. If the elevation of serum tumor markers is not straightforward indicating malignancy, surgical removal is recommended [78, 79].

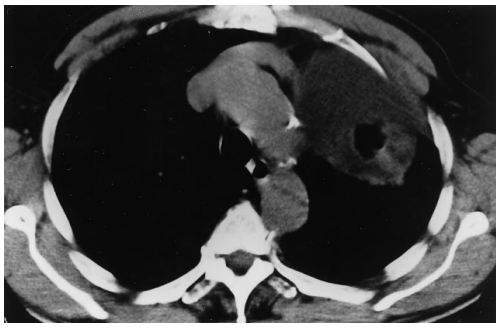

Fig. 9. CT scan of Benign teratoma. Mixture of fatty, water, and solid tissular densities

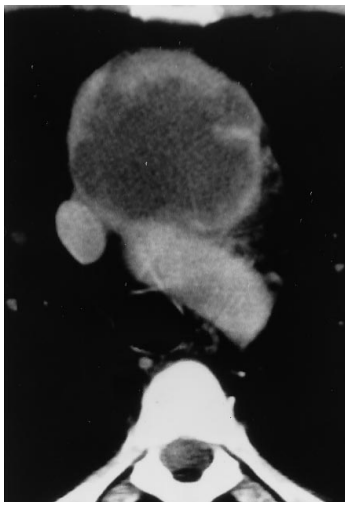

Fig. 10. CT scan of necrotic choriocarcinoma. Large low-density mass with a thick wall in the anterior mediastinum

Neurogenic tumors

Neural tumors can be divided into nerve sheath tumors, ganglion cell tumors, and paraganglionic cell tumors. The latter have been discussed previously. The nerve sheath tumors comprise schwannomas, neurofibromas, and their malignant counterpart. All of them are common in neurofibromatosis. Schwannoma is eccentric and encapsulated and has no nerve fibers passing through it, whereas neurofibroma is unencapsulated and has nerve fibers scattered through the tumor. Almost all intrathoracic nerve sheath tumors arise from either the intercostal or the sympathetic nerves, with some exceptions arising from the phrenic or vagus nerves. Most nerve sheath tumors are benign and asymptomatic, and are rare in people under 20 years. Ganglion cell tumors form a spectrum: neuroblastomas are the malignant form and ganglioneuromas the benign form. They are essentially childhood tumors with 10% occuring in subjects over 20.

Chest radiography typically shows a sharply circumscribed round or oval mass located in the paravertebral gutter when the tumor arises from the nerve sheath. When arising from ganglial cells, they are more anteriorly located. Rib erosion with a sclerotic border is suggestive of a benign lesion. Spreading to multiple ribs

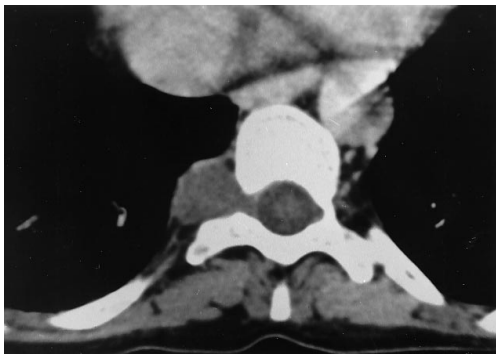

Fig. 11. Neurinoma. Homogeneous low-density mass of the paravertebral gutter. An extension into the neural foramen is suspected suggesting a neural tumor

with erosion or destruction is in favor of malignancy. Calcification may be seen in all types of neural tumors.

On CT scans neurogenic tumors have a tissular density but may show a low-attenuation value attributed to lipid content, cystic degeneration, and entrapment of peripheral neural tissue (Fig. 11) [80]. Relationships with vertebrae, ribs, and the spinal canal are essential for planning therapy [81, 82].

At MRI neurofibromas may show a so-called target pattern with a lower signal intensity in the central por-

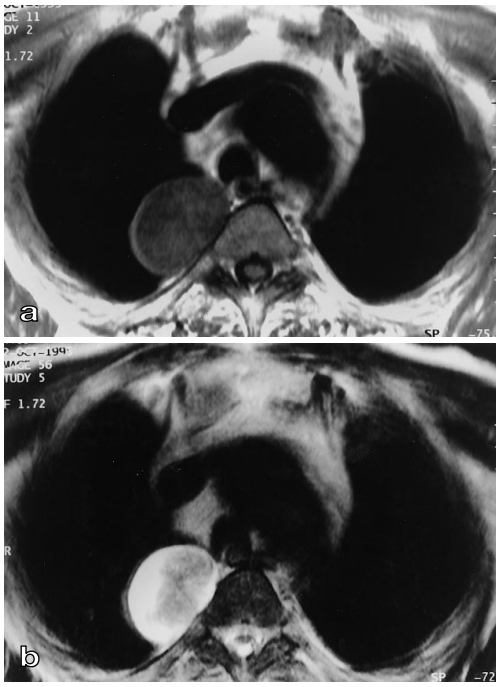

Fig. 12 a, b. MRI of neurinoma. Mass of the paravertebral gutter of low signal intensity on **a** T1-weighted image, and target appearance on **b** T2-weighted image

Fig. 13. Enhanced MRI, frontal view, of dumbbell neurinoma. Large enhancing mass extending throughout the vertebral foramen in the subarachnoidal space

tion compared with the peripheral zone on T2-weighted images (Fig. 12). Other types of neural tumors do not show this feature [83]. Schwannomas may show inhomogeneity on T2-weighted images and on T1-weighted images after gadolinium injection. This is related to various tissue components, vascularity, or cystic degeneration. Magnetic resonance imaging can demonstrate spinal involvement without the use of intrathecal contrast material (Fig. 13). Moreover, its multiplanar capabilities help in demonstrating the longitudinal spread along the spine.

Plexiform neurofibromas, pathognomonic of von Recklinghausen's disease, occur virtually in any location. In the thorax the sympathetic chains are most commonly involved, but the vague and phrenic nerves can be affected. The CT technique shows multiple low-attenuation lesions and MRI is particularly accurate for demonstrating the spread of the disease [84].

A diverse group of entities different from neurogenic tumors may also involve the posterior mediastinum, including lipomatosis, lymphadenopathies, aortic aneurysm, cystic masses, and thoracic spinal inflammatory or neoplastic lesions. Computed tomography is often diagnostic, but MRI has one of its best indications [9, 10].

Fibrous and sarcomatous tumors

Desmoid tumors, also known as aggressive fibromatosis, are locally invasive tumors that are very rarely found in the mediastinum. Sarcomas other than vascular neural or lyomatous origin, including fibrosarcomas, osteosarcomas, and chondrosarcomas, are also very uncommon, some arising from the chest wall. They show non-specific appearance, but some dense areas of calcification or ossification are in favor of the latter.

References

1. Davis RD, Oldham NH, Sabiston DC (1987) Primary cysts and neoplasms of the mediastinum: recent changes in clinical presentation, methods of diagnosis, management and results. Ann Thorac Surg 44: 229–37
2. Cohen AJ, Thompson LN, Edwards FH, Bellamy RF (1991) Primary cysts and tumors of the mediastinum. Ann Thorac Surg 51: 378–86
3. Azarow KS, Pearl RH, Zurcher R, Edwards FH, Cohen AJ (1993) Primary mediastinal masses. A comparison of adult and pediatric populations. J Thorac Cardiovasc Surg 106: 67–72
4. Tecce PM, Fishman EK, Kuhlman JF (1994) CT evaluation of the anterior mediastinum: spectrum of disease. Radiographics 14: 973–990
5. Kohman LI (1993) Approach to the diagnosis and staging of mediastinal masses. Chest 103: 328S–330S
6. Rice TW (1992) Benign neoplasms and cysts of the mediastinum. Sem Thorac Cardiovasc Surg 4: 25–33
7. Fraser RG, Paré PJA, Paré PD, Fraser RS, Généreux GP (1991) Diseases of mediastinum in diagnosis of diseases of the chest. Saunders, Philadelphia, pp 2814–1910
8. Heitzman ER (1988) The mediastinum: radiologic correlations with anatomy and pathology. Springer, Berlin Heidelberg New York, pp 7–309
9. Naidich DP, Zerhouni EA, Siegelman SS (1991) Mediastinum in computed tomography and magnetic resonance of the thorax. Raven Press, New York, pp 36–148
10. Armstrong P (1995) Mediastinal and hilar disorders. In: Armstrong P, Wilson AG, Dee P, Hansell DM (eds) Imaging of diseases of the chest. Mosby, St. Louis, pp 717–816
11. Ikezoe J, Takeuchi N, Johkoh T, Kohno N, Takashima S, Tomiyama N, Arisawa J, Yamagami H, Yoshioka H, Higashihara T (1992) MRI of anterior mediastinal tumors. Radiat Med Imaging Radiat Oncol 10: 176–183
12. Webb WR, Sostman HD (1992) MRI imaging of thoracic disease: clinical uses. Radiology 182: 621–630
13. Link KM, Samuels LJ, Reed JC, Loehr SP, Lesko NM (1993) Magnetic resonance imaging of the mediastinum. J Thorac Imaging 8: 34–53
14. Wernecke K, Vassallo P, Pöetter R, Lückener HG, Peters PE (1990) Mediastinal tumors: sensitivity of detection with sonog-

raphy compared with CT and radiography. Radiology 175: 137–143
15. Yu CT, Yang PC, Chang DR, Wu HD, Lee LN, Lee YC, Kuo SH, Luh KT (1991) Evaluation of ultrasonically guided biopsies of mediastinal masses. Chest 100: 399–405
16. D'Agostino HB, Sanchez RB, O'Laoide RM, Oglevie S, Donaldson JS, Russack V, Gonzalez Villaveiran R, vanSonnenberg E (1993) Anterior mediastinal lesions: transsternal biopsy with CT guidance. Radiology 189: 703–705
17. Woodring JH, Johnson PJ (1991) Computed tomography distinction of central thoracic masses. J Thorac Imaging 6: 32–39
18. Rodriguez E, Soler R, Gayol A, Freire R (1995) Massive mediastinal and cardiac fatty infiltration in a young patient. J Thorac Imaging 10: 225–226
19. Ferretti G, Pittet L, Pison C, Ranchoup Y, Le March'Hadour F, Sarrazin R, Coulomb M (1992) Liposarcome primitif du médiastin: apport de l'IRM au diagnostic. A propos d'un cas. Rev Mal Resp 9: 467–469
20. Rosado-de-Christenson M, Pugatch RD, Moran CA, Galobardes J (1994) Thymolipoma: analysis of 27 cases. Radiology 193: 121–126
21. Kline ME, Patel BU, Agosti SJ (1990) Noninfiltrating angiolipoma of the mediastinum. Radiology 175: 737–738
22. Federici S, Cuoghi D, Sciutti R (1992) Benign mediastinal lipoblastoma in a 14-month-old infant. Pediatr Radiol 22: 150
23. Savader SJ, Otero RR, Savader BL (1988) MR imaging of intrathoracic extramedullary hematopoiesis. J Comput Assist Tomogr 12: 878–880
24. Stark P, Eber CD, Jacobson F (1994) Primary intrathoracic malignant mesenchymal tumors: pictorial essay. J Thorac Imaging 9: 148–155
25. Glazer HS, Siegel MJ, Sagel SS (1989) Low-attenuation mediastinal masses on CT. AJR 152: 1173–1177
26. Glazer HS, Molina PK, Siegel MJ, Sagel SS (1991) High-attenuation mediastinal masses on unenhanced CT. AJR 156: 45–50
27. Murayama S, Murakami J, Watanabe H, Sakai S, Hinaga S, Soeda H, Nakata H, Masuda K (1995) Signal intensity characteristics of mediastinal cystic masses on T1-weighted MRI. J Comput Assist Tomogr 19: 188–191
28. St-Georges R, Deslauriers J, Duranceau A, Vaillancourt R, Deschamps C, Beauchamp G, Pagé A, Brisson J (1991) Clinical spectrum of bronchogenic cysts of the mediastinum and lung in the adult. Ann Thorac Surg 52: 6–13
29. Suen HC, Mathisen DJ, Grillo HC, LeBlanc J, McLoud TC, Moncure AC, Hilgenberg AD (1993) Surgical management and radiological characteristics of bronchogenic cysts. Ann Thorac Surg 55: 476–481
30. Naidich DP, Rumancik WM, Ettenger NA, Feiner HD, Harnanz-Schulman M, Spatz EM, Toder ST, Genieser NB (1988) Congenital anomalies of the lungs in adults: MR diagnosis.
31. Nakata H, Egashira K, Watanabe H, Nakamura K, Onitsuka H, Murayama S, Murakami J, Masuda K (1993) MRI of bronchogenic cysts. J Comput Assist Tomogr 17: 267–270
32. Palmer WE, Rivitz SM, Chew FS (1991) Bilateral bronchogenic cysts. AJR 157: 950
33. Lyon RD, McAdams HP (1993) Mediastinal bronchogenic cyst: demonstration of a fluid–fluid level at MR imaging. Radiology 186: 427–428
34. Bargallo J, Luburich P, Garcia-Barrionuevo J, Sanchez-Gonzalez M (1993) Fluid–fluid level in bronchogenic cysts. Radiology 188: 881–882
35. Vinne P, Stover R, Sigmund G, Laubenberger J, Hauenstein KH, Weyrig G, Hennig J (1992) MR imaging of the pericardial cyst. J Magn Reson Imaging 2: 593–596
36. Kostopoulos GK, Fessatidis JT, Hevas AL, Skordalaki AS, Spyrou PG (1993) Mediastinal cystic hygroma: report of a case with review of the literature. Eur J Cardiovasc Thorac Surg 7: 166–167
37. Pannell TL, Jolles H (1991) Adult cystic mediastinal lymphangioma simulating a thymic cyst. J Thorac Imaging 7: 86–89
38. Miyake H, Shiga M, Takaki H, Hata H, Onishi R, Mori H (1996) Mediastinal lymphangiomas in adults: CT findings. J Thorac Imaging 11: 83–85
39. Kobayashi H, Furuse M, Yamada T, Mukai M (1994) Cavernous lymphangioma of the thorax: MRI findings. J Thorac Imaging 9: 64–66
40. Shaffer K, Rosado-de-Christenson ML, Patz EF, Young S, Farver CF (1994) Thoracic lymphangioma in adults: CT and MR imaging features. AJR 162: 283–289
41. Lamers RJS, Belle AF (1993) Thoracic duct cyst in the middle part of the mediastinum. AJR 161: 675
42. Schulthess GK von, Baumann R, Weder W, Duewell S (1993) MRI, CT, sonography and thallium-technetium subtraction scintigraphy for the detection of parathyroid disease: a four-year experience. Eur Radiol 3: 71–76
43. Higgins CB (1993) Role of magnetic resonance imaging in hyperparathyroidism. Radiol Clin North Am 31: 1017–1028
44. Kang YS, Rosen K, Clark O, Higgins CB (1993) Localization of abnormal parathyroid glands of the mediastinum with MR imaging. Radiology 189: 137–141
45. McDermott VG, Mendez Fernandez RJ, Meakem TJ, Stolpen AH, Spritze CE, Gefter WB (1996) Preoperative MR imaging in hyperparathyroidism: results and factors affecting parathyroid detection. AJR 166: 705–710
46. Stevens SK, Chang JM, Clark OH, Chang PJ, Higgins CB (1993) Detection of abnormal parathyroid glands in postoperative patients with recurrent hyperparathyroidism: sensitivity of MR imaging. AJR 160: 607–612
47. Doppman JL, Skarulis MC, Chen CC, Chang R, Pass HI, Fraker DL, Alexander HR, Niederle B, Marx SJ, Norton JA, Wells SA, Spiegelv AM (1996) Parathyroid adenomas in the aortopulmonary window. Radiology 201: 456–462
48. Perez-Monte JE, Brown ML, Shah AN, Ranger NT, Watson CG, Carty SE, Clarke MR (1996) Parathyroid adenomas: accurate detection and localization with Tc-99 m Sestamibi SPECT. Radiology 201: 85–91
49. Moon KW, Im JG, Kim JS, Choi CG, Kim HC, Yeon KM, Han MC (1994) Mediastinal Castelman disease: CT findings. J Comput Assist Tomogr 18: 43–46
50. Ecklund K, Hartnell GG (1994) Mediastinal Castelman disease: MR and MRA features. J Thorac Imaging 9: 156–159
51. Moon KW, Im JG, Kim JS, Choi CG, Kim HC, Yeon KM, Han MC (1994) Mediastinal Castelman disease: CT findings. J Comput Assist Tomogr 18: 43–46
52. Moran CA, Suster S, Fishback N et al. (1993) Mediastinal paragangliomas: a clinico-pathologic and immunohistochemical study of 16 cases. Cancer 72: 2358–2364
53. Cornford EJ, Wastie ML, Morgan DAL (1992) Malignant paraganglioma of the mediastinum: a further diagnostic and therapeutic use of radiolabelled MIBG. Br J Radiol 65: 75–78
54. Page McAdams H, Rosado-de-Christenson M, Moran CA (1994) Mediastinal hemangioma: radiographic and CT features in 14 patients. Radiology 193: 399–402
55. Francis IR, Glazer GM, Bookstein FL, Gross BH (1995) The thymus: reexamination of age-related changes in size and shape. AJR 145: 249–254
56. Brown LR, Muhm JF, Sheedy PF II, Hermann RC Jr (1993) The value of computed tomography in myasthenia gravis. AJR 140: 31–35
57. Nicolaou S, Müller NL, Li DKB, Oger JJF (1996) Thymus in myasthenia gravis: comparison of CT and pathologic findings and clinical outcome after thymectomy. Radiology 201: 471–474
58. Chen J, Weisbrod GL, Herman SJ (1988) Computed tomography and pathologic correlations of thymic lesions. J Thorac Imaging 3: 61–65
59. Rosado-de-christenson M, Galobardes J, Moran CA (1992) Thymoma: radiologic–pathologic correlation. Radiographics 12: 151–168
60. Molina PL, Siegel MJ, Glazer HS (1990) Thymic masses on MR imaging. AJR 155: 495–500

61. Sakai F, Sone S, Kiyono K, Kawai T, Maruyama A, Ueda H, Jaoki J, Honda T, Morimoto M, Ishii K, Ikeda S (1992) MR imaging of thymoma: radiologic–pathologic correlation. AJR 158: 751–756
62. Doo Lee J, Choe KO, Kim SJ, Kim GE, Im JG, Lee JT (1991) CT findings in primary thymic carcinoma. J Comput Assist Tomogr 15: 429–433
63. Hsu CP, Chen CY, Chen CL, Lin CT, Hsu NY, Wang JH, Wang PY (1994) Thymic carcinoma. Ten year's experience in twenty patients. J Thorac Cardiovasc Surg 107: 615–620
64. Do YS, Im JG, Lee BH, Kim KH, Oh YW, Chin SY, Zo JI, Jang JJ (1995) CT findings in malignant tumors of thymic epithelium. J Comput Assist Tomogr 19: 192–197
65. Quagliano PV (1996) Thymic carcinoma: case reports and review. J Thorac Imaging 11: 66–74
66. Wang DY, Chang DB, Kuo SH, Yang PC, Lee YC, Hsu HC, Luh KT (1994) Carcinoid tumors of the thymus. Thorax 49: 357–360
67. Choyke P, Zeman R, Gootenberg J, Greenberg J, Hoffer F, Joseph F (1987) Thymic atrophy and regrowth in response to chemotherapy: CT evaluation. AJR 149: 269–272
68. Kissin C, Husband J, Nicholas D, Eversman W (1987) Benign thymic enlargement in adults after chemotherapy: CT demonstration. Radiology 163: 67- 70
69. Wenger MC, Cohen AJ, Greensite F (1994) Thymic rebound in a patient with scrotal mesothelioma. J Thorac Imaging 9: 145–147
70. Dehner LP (1990) Germ cell tumors of the mediastinum. Semin Diagn Pathol 7: 266–284
71. Rosado-de-Christenson ML, Templeton PA, Moran CA (1992) From the archives of the AFIP. Mediastinal germ cell tumors: radiologic and pathologic correlation. Radiographics 12: 1013–1030
72. Quillin SP, Spiegel MJ (1992) CT features of benign and malignant teratomas in children. J Comput Assist Tomogr 16: 722–726
73. Fulcher AS, Proto AV, Jolles H (1990) Cystic teratoma of the mediastinum: demonstration of fat/fluid level. AJR 154: 259–260
74. Yeoman LJ, Dalton HR, Adam FJ (1990) Fat–fluid level in pleural effusion as a complication of a mediastinal dermoid: CT characteristics. J Comput Assist Tomogr 14: 307–309
75. Nichols CR, Saxman S, Williams SD, Loehrer PJ, Miller ME, Wright C, Einhorn L (1990) Primary mediastinal nonseminomatous germ cell tumors. Cancer 65: 1641–1646
76. Saxman S, Nichols CR, Williams S, Loehrer P, Einhorn LH (1991) Mediastinal yolk sac tumor. J Thorac Cardiovasc Surg 102: 913–916
77. Dulmet EM, Macchiarini P, Suc B, Verley JM (1993) Germ cell tumors of the mediastinum. Cancer 72: 1894–1901
78. Panicek DM, Toner GC, Heelan RT, Bosl GJ (1990) Nonseminomatous germ cell tumors: enlarging masses despite chemotherapy. Radiology 175: 499–502
79. Chen LT, Chen CL, Hwang WS (1990) The growing teratoma syndrome. A case of primary mediastinal nonseminomatous germ cell tumor treated with chemotherapy and radiotherapy. Chest 98: 231–233
80. Kawashima A, Fishman EK, Kuhlman JF, Nixon MS (1991) CT of posterior mediastinal masses. Radiographics 11: 1045–1067
81. Moon WK, Im JG, Han MC (1993) Malignant schwannomas of the thorax: CT findings. J Comput Assist Tomogr 17: 274–276
82. Ribet ME, Cardot GR (1994) Neurogenic tumors of the thorax. Ann Thorac Surg 58: 1091–1095
83. Suh JS, Abenoza P, Galloway H, Everson LI, Griffiths HJ (1992) Peripheral (extracranial) nerve tumors: correlation of MR imaging and histologic findings. Radiology 183: 341–346
84. Bourgouin PM, Shepard JAO, Moore EH, McLoud TC (1988) Plexiform neurofibromatosis of the mediastinum: CT appearance. AJR 151: 461–463

Book review

European Radiology

Bauer, B. L., Kuhn, T. J.: Severe Head Injuries: Pathology, Diagnosis and Treatment. Berlin, Heidelberg, New York: Springer 1997. 154 pp., 15 figures, 6 tables, (ISBN 3-540-62701-4), DM 128.00.

This book is the result of a project on the management and outcome of brain-injured patients. The 15 chapters are all written by different authors. The importance of a multidisciplinary approach is stressed in the preface as can be seen from the unfortunately incomplete list of contributors belonging to many different disciplines. The book covers the different aspects of neurotraumatology.

The first brief chapter reviews clinical head injury trials. The second and third chapters deal with pathophysiology and morphology of brain injury. The preclinical management is discussed in Chapters 4 and 5. There is some overlap between Chapters 4, 5 and 7 which could have easily been summarized in one chapter. Chapter 6 reviews all aspects of carotid cavernous fistulas. In Chapter 7 guidelines are given for the treatment of head injury. Fractures are discussed in Chapters 8 and 9. The paragraph on "diagnosis" in Chapter 8 is very short and contains some inaccuracies. The authors refer to the new technique of MR cisternography but their comment is rather poor and they fail to provide a reference. In Chapter 10 the pathophysiology of cranial trauma is discussed. Chapter 11 deals with intracranial hypertension in children. The remaining chapters, except Chapter 14, are devoted to the monitoring and outcome of brain injury. Chapter 14 discusses cranial nerve palsy after trauma.

There is a difference in style as can be expected from a multiauthored book and some chapters are not always logical and concise. Recent references (updated to 1997!) are listed at the end of the chapters for the interested reader.

The quality of printing and photographic reproduction is good. The price is rather elevated for the amount of pages that is offered. This book is a mixture of chapters reviewing the pathophysiological mechanisms that occur during and after cranial trauma (Chapters 2–8, 10, 11 and 14) and chapters presenting the clinical results of the author(s) (Chapters 9, 12, 13 and 15). Overall, little attention is paid to the radiological aspects. Therefore, I cannot recommend this book to radiologists, who would probably benefit more from a book on imaging of head trauma that is already on sale. The book that is reviewed here should be considered rather as a valuable addition for radiologists who have a particular interest in cranial trauma.

P. Demaerel, Leuven